Acta Crystallographica Section B
Structural Science
ISSN 0108-7681

Crystal structure study of a β'-copper vanadium bronze, $Cu_xV_2O_5$ (x = 0.63), by X-ray and convergent beam electron diffraction

Victor A. Streltsov,[a]* Philip N. H. Nakashima,[b] Alexandre N. Sobolev[c] and Ruslan P. Ozerov[b]

[a]CSIRO HSN, 343 Royal Parade, Parkville, Victoria 3052, Australia, [b]School of Physics and Materials Engineering, Monash University, Clayton, Victoria 3800, Australia, [c]University of Western Australia, Crawley, WA 6009, Australia, and [d]Mendeleev University of Chemical Technology of Russia, Moscow 125047, Russia

Correspondence e-mail: victor.streltsov@csiro.au

Received 12 August 2004
Accepted 29 October 2004

The single-crystal structure of a β'-copper vanadium bronze, $Cu_{0.63}V_2O_5$, has been studied at room temperature and 9.6 K, and compared with that of the β-sodium vanadium bronze, $Na_{0.33}V_2O_5$, structure. No convincing evidence to oppose an assignment of centrosymmetric $C2/m$ symmetry to the structure was identified using the X-ray data. A subsequent convergent beam electron diffraction (CBED) experiment was performed and confirmed the $C2/m$ space group. The oxygen–vanadium atom framework of $Cu_{0.63}V_2O_5$ is close to that of $Na_{0.33}V_2O_5$. However, in the copper compound the Cu atoms are located in two positions: Cu1 in the 4(i) position with x = 0.541, y = 0 and z = 0.345, and Cu2 in the 8(j) position with x = 0.529, y = 0.038 and z = 0.357. The crystal structure changes little with temperature. Disorder of the Cu ion over two sites is seen at 9.6 K. This suggests that distribution of the Cu atoms over two sites is of a more static than dynamic nature.

1. Introduction

The vanadium bronzes β- and β'-$M_xV_2O_5$ (x varies from 0.2 to 0.8, and M = Na, Ca, Sr, Pb, Cu or Fe) exhibit a variety of phenomena originating from strong electron correlations. These compounds have recently gained increased interest, firstly because of the discovery of superconductivity under high pressures in β-$Na_{0.33}V_2O_5$ at 8 GPa and T_c = 8 K (Yamauchi *et al.*, 2002), and in β'-$Cu_{0.65}V_2O_5$ at 3 GPa and T_c = 6 K (Ueda *et al.*, 2002). The superconductivity in the vanadium bronzes occurred in the quasi-one-dimensional conducting state, similar to organic superconductors. Secondly, new applications of bronzes as rechargeable electrodes (Shacklette *et al.*, 1988) and ion-selective devices (Smirnova *et al.*, 2003) have been proposed.

The difference between β- and β'-phases is related to the M-atom content and its positions, giving a theoretical upper limit of x = 0.33 and 0.66 in the β- and β'-phases, respectively. The β- and β'-phases are characterized by similar V_2O_5 networks with three independent vanadium sites. The V1 and V3 atoms form zigzag-type double chains along the b axis composed of the edge-shared $V1O_6$ octahedra and $V3O_5$ square pyramids, respectively. In contrast, the V2 atoms form a two-leg ladder composed of corner-shared $V2O_6$ octahedra along the b axis. After the first crystal structure determination of $Na_xV_2O_5$, archetypal of the whole family of β-vanadium oxide bronzes (Wadsley, 1955), a dozen new bronzes have been synthesized and their structures investigated. Some of them have the same crystal structure as $Na_xV_2O_5$ (*e.g.* $K_xV_2O_5$; Ozerov *et al.*, 1957). However, there are some species with different locations of metal ions in the V—O framework channels. For example, the Ag atoms in $Ag_xV_2O_5$ are found to occupy two sites in the

Table 1
Experimental details.

Crystal data	
Chemical formula	$Cu_{0.63}O_5V_2$
M_r	221.59
Cell setting, space group	Monoclinic, *C*2/*m*
a, *b*, *c* (Å)	15.100 (1), 3.6382 (2), 10.0595 (7) 15.186 (1), 3.6365 (3), 19.0882 (9)†
β (°)	105.585 (6) 106.049 (7)†
V (Å^3)	532.32 (6)
Z	6
D_x (Mg m^{-3})	4.147
Radiation type	Mo $K\alpha$
No. of reflections for cell parameters	16
θ range (°)	2.1–50.12
μ (mm^{-1})	8.79
Temperature (K)	9.6 (5)
Crystal form, colour	Rectangular, black
Crystal size (mm)	0.27 × 0.18 × 0.17
Data collection	
Diffractometer	HUBER 512
Data collection method	$\omega/2\theta$
Absorption correction	Analytical
T_{min}	0.2682
T_{max}	0.3809
No. of measured, independent and observed reflections	11 127, 3051, 3041
Criterion for observed reflections	$F > 0.00\sigma(F)$
R_{int}	0.021
θ_{max} (°)	50.0
Range of *h*, *k*, *l*	$-32 \Rightarrow h \Rightarrow 32$ $-7 \Rightarrow k \Rightarrow 7$ $-21 \Rightarrow l \Rightarrow 21$
Intensity decay (%)	1
Refinement	
Refinement on	*F*
$R[F^2 > 0\sigma(F^2)]$, $wR(F^2)$, *S*	0.018, 0.019, 2.65
No. of reflections	3041
No. of parameters	83
Weighting scheme	Based on measured s.u.'s
$(\Delta/\sigma)_{max}$	1.956
$\Delta\rho_{max}$, $\Delta\rho_{min}$ (e Å^{-3})	0.77 (7), −1.78 (7)
Extinction method	Zachariasen
Extinction coefficient	23 300 (300)

Computer programs used: *Xtal DIFDAT ADDREF ABSORB SORTRF*, *Xtal*, *Xtal CRYLSQ*, *Xtal CIFIO* (Hall *et al.*, 2000). † Cell parameters at room temperature.

channels at the same level as the Na site in the sodium compound. This changes the upper bound of the silver content ($0.29 \leq x \leq 0.41$; Déramond *et al.*, 1994). Another distribution of Fe ions has been found in the iron bronze, $Fe_{0.33}V_2O_5$ (Permer & Ferey, 1994), which is expected to be close to that of Cu in copper bronze.

The copper bronze phase was denoted as a β' phase and the first structure of this kind was obtained for $Li_xV_2O_5$ (Hardy *et al.*, 1965). In the sodium compound the Na atoms occupy positions in an alternating manner in the vanadium–oxygen tunnels of the bicapped trigonal prism, whereas in the copper compound the Cu atoms are supposed to be displaced from the centres of pyramids to their tops (trigonal faces) along the monoclinic axis by *b*/2. Galy *et al.* (1970) assigned the crystal structure of $Cu_{0.55}V_2O_5$ at room temperature to the non-centrosymmetric space group *Am* with two independent Cu atoms: one of them was located in the mirror plane whereas the other was placed out of that plane. On the other hand, Kato *et al.* (1989) reported the crystal structure of $Cu_{0.261}V_2O_5$, at room temperature, to belong to the centrosymmetric space group *C*2/*m* with one crystallographic site for the Cu atoms. However, these authors identified residual electron density peaks around the Cu-atom sites, which they attributed entirely to the anharmonicity of the Cu-atom thermal vibrations. A recent low-temperature single-crystal X-ray study of vanadium oxide bronzes including $Cu_{0.65}V_2O_5$ (Yamaura *et al.*, 2002) revealed additional reflections related to the *C*2/*m* symmetry breaking at $T < 255$ K. Unfortunately, the final structural refinement using data at $T = 120$ K in the proposed $P2_1/m$ space group showed unreliable statistics: $R(wR) = 0.064$ (0.194).

Although a variety of studies have already been conducted (see Savariault *et al.*, 1994, and references therein; Popovic *et al.*, 2003; citations in Ozerov *et al.*, 2001), the properties of bronzes are not yet fully understood due to their complex electronic and crystal structure. Whilst several studies of β'-phases have been undertaken, there is no consensus about the space-group symmetry and the cation metal sub-structure. Therefore, we have conducted the space-group determination and structural study of a copper bronze crystal with the composition $Cu_{0.63}V_2O_5$ at room temperature and 9.6 K. In order to discriminate between enantiomorphic models, some statistical tests, as proposed by Abrahams *et al.* (1998), have been attempted using the X-ray diffraction data. Furthermore, the convergent beam electron diffraction (CBED) method was employed to check the crystal symmetry in a number of crystallites taken from the same batch used for the X-ray diffraction experiment. Goodman (1975, 2001) gave authoritative descriptions on symmetry determination in crystals by CBED, which is a very sensitive probe of localized crystal structure.

2. Experimental

2.1. X-ray diffraction

The room- and low-temperature data sets were measured at the Department of Chemistry, University of Western Australia, with a locally assembled Huber 512 goniometer equipped with a Displex 202D cryogenic refrigerator. Attempts were made at low temperature to find superstructure reflections arising from *b*-axis doubling. A scan along the 0*y*0 direction showed no additional peaks between the principal reflections, that is no *b*-axis doubling was found at the experimental temperatures of 300 and 9.6 K. Temperature changes do not significantly affect the crystal structure. The *b*-cell parameter was almost constant, whereas the *a* and *c* parameters were reduced, as expected, at low *T* (Table 1).[1] From hereon we will only focus on the 9.6 K data.

Reflection intensities spanning a whole sphere were measured to $(\sin\theta/\lambda)_{max} = 1.08$ Å^{-1} using β-filtered Mo X-rays

[1] Supplementary data for this paper are available from the IUCr electronic archives (Reference: AV5018). Services for accessing these data are described at the back of the journal.

Table 2
Observed mean-normalized structure factors and expected values for randomly distributed centrosymmetric and non-centrosymmetric structures.

	$\|E\|$	$\|E^2\|$	$\|E^2-1\|$	$\|E^2-1\|^2$	$\|E^2-1\|^3$
Random $P\bar{1}$	0.798	1.000	0.968	2.000	8.000
For $\|E1\|$ estimate	0.817	1.000	0.933	1.661	5.275
For $\|E2\|$ estimate	0.818	1.000	0.930	1.650	5.219
Random $P1$	0.886	1.000	0.736	1.000	2.000

and a $\omega/2\theta$ scan procedure based on locally written diffractometer control software. The correction for absorption by the beryllium shield was performed by the *PROFIT* (Streltsov & Zavodnik, 1989) program and the analytical crystal absorption correction and structure refinements were conducted with *Xtal*3.7 (Hall *et al.*, 2000). Further experimental conditions and crystal data for $Cu_{0.63}V_2O_5$ at 9.6 K are given in Table 1.

The systematic extinctions and diffraction symmetry of the $Cu_{0.63}V_2O_5$ crystals were consistent with three space groups belonging to the same Laue class (centrosymmetric $C2/m$ and non-centrosymmetric Cm and $C2$). Additionally, we have attempted discrimination of the space groups using statistical tests and CBED.

2.2. Space-group assessment

A simple method for discriminating between centrosymmetric and non-centrosymmetric structures is to compare the observed distribution of normalized, experimentally measured structure factors with those calculated using randomly distributed atoms in centrosymmetric or non-centrosymmetric symmetries (see *e.g.* Shmueli & Wilson, 1993, and references therein). Table 2 shows the observed and expected mean values from random estimates. The experimental values lie midway between the theoretical $P1$ and $P\bar{1}$ symmetry values, making this test inconclusive. This is most likely due to the formal requirements for statistical tests, such as an equal-atom structure and atoms in general positions, not being exactly observed.

The enantiomorphic models can also be distinguished in least-squares processes by refining the absolute structure parameter (Flack, 1983). The Flack parameter is determined by minimizing a residual based on the differences arising from the complex component of the dispersion correction between Friedel-pair structure factors. Table 3 shows the results of the structure refinements for non-centrosymmetric Cm and $C2$ space groups. The Flack parameter converged to the values of 0.50 (4) and 0.50 (3), respectively, suggesting that the structure can be either centrosymmetric or a non-centrosymmetric inversion twin. Further, the value of the standard uncertainty (s.u.) in the Flack parameter may indicate that the crystal is not enantiopure (Flack & Bernardinelli, 2000). However, the structural refinements in non-centrosymmetric groups with an increased number of adjustable parameters showed markedly worse convergence and higher correlation between parameters compared with the centrosymmetric space-group refinement (Table 3). The Flack parameter's s.u. can be significantly underestimated in such ill-conditioned least-squares optimizations according to Flack & Bernardinelli (2000). In this case the Flack parameter cannot be interpreted reliably.

Table 3
Refinement statistics and Flack parameter values for different space-group symmetries.

Space group	$C2/m$	Cm	$C2$
No. of parameters, p	83	154	117
No. of reflections, n	3041	3039	3037
S	2.651	3.092	3.042
R	0.018	0.021	0.022
wR	0.019	0.022	0.021
Flack parameter		0.50 (4)	0.50 (3)

In the absence of conclusive statistical evidence from the X-ray diffraction component of this work, a symmetry study using CBED was initiated, the details of which are given in the following section.

2.3. CBED symmetry determination

CBED is a well established technique for very sensitively determining crystal symmetry (Goodman, 1975, 2001). The sensitivity stems from the very strong interaction of electrons with the crystal potential, which results in strong dynamic (multiple) scattering from specimens thicker than a few hundred Å. CBED measurements are highly localized as modern electron microscopes can easily form nanometre-sized convergent beam electron probes. Dynamic diffraction allows the resolution of the structure factor phase and violations of Friedel's law because the multiple scattering pathways give rise to reflection couplings which are sensitive functions of their structure factor phases. The bonus of the technique is that two-dimensional rocking curves for each reflection in a CBED pattern show the intensity distribution over the angle of the converged probe. This allows symmetry determination by visual inspection of zone axis and near-zone axis CBED patterns rather than measuring integrated intensities, as is the case in parallel-beam experiments.

The most direct space-group test for the present material, given the results obtained so far from X-ray diffraction, is one that attempts to find the twofold axis and the mirror plane in the proposed $C2/m$ model of the crystal structure. CBED experiments were performed using a small quantity of crystals from the same batch used for single-crystal X-ray diffraction. Specimens were prepared by crushing a few crystals with an agate pestle and mortar, and suspending the fragments in ethanol. The suspension was then transferred to a copper transmission electron microscope (TEM) specimen grid (200 mesh) coated with holey carbon support film. CBED patterns were collected at electron energies of 160 and 200 keV.

Fig. 1 shows a diffraction pattern captured at 200 keV with the incident electron beam oriented along the [203] zone axis. It shows the preservation of the three-dimensional mirror in three higher-order Laue zones (HOLZ) as well as the zero-order Laue zone (ZOLZ). The whole-pattern symmetry of m

proves there is a mirror plane in the three-dimensional crystal structure (as opposed to a mirror in the two-dimensional structure projected along [203]). This leaves only *C*2/*m* and *Cm* as possible space groups. The ZOLZ reveals information about the crystal structure in projection along the direction of the incident beam, whilst HOLZ information reveals the symmetry of the three-dimensional structure in that direction (Goodman, 1975, 2001). The second part of Fig. 1 shows the ZOLZ component of the pattern without the central beam. The central beam contains all intensity deficiencies due to scattering into all other beams and therefore echoes the whole pattern symmetry. A consideration of only the ZOLZ reflections (minus the central beam) shows 2*mm* symmetry in the projected crystal structure in this direction, allowing for the much weaker HOLZ deficiencies in the ZOLZ reflections. The model for the *C*2/*m* structure in the [203] direction is given above the pattern in Fig. 1, showing the mirror plane in the three-dimensional structure, while the model in projection is given next to the extracted ZOLZ pattern. The projected 2*mm* symmetry is evident in both the model and the ZOLZ component of the [203] zone axis CBED pattern.

Fig. 2 shows a CBED pattern collected at 200 keV from the [010] zone axis, *i.e.* along the short *b* axis in the structure. Only the ZOLZ with its twofold symmetry is shown because a very long exposure at a very low camera length failed to register the presence of the first-order Laue zone (FOLZ, because of the very short *b* axis). The absence of HOLZ information only allows a conclusion that the *b*-axis is twofold in projection from this pattern alone. However, Fig. 1 implies that [010] must be a twofold axis in three dimensions, otherwise there would be no 2*mm* symmetry in the projected structure along [203]. The second mirror in the projected structure shown in Fig. 1 is parallel to the *b* axis and can therefore only exist if the *b* axis is a true twofold axis in the three-dimensional structure. The combination of Figs. 1 and 2 leads to the conclusion that the $Cu_{0.63}V_2O_5$ crystal structure has centrosymmetric *C*2/*m* symmetry.

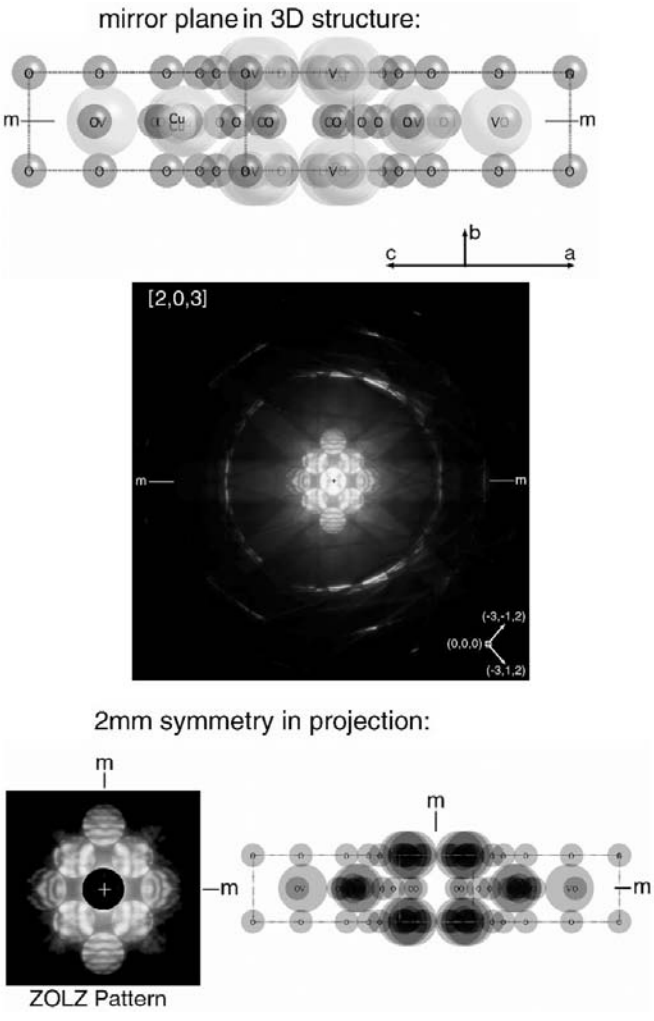

Figure 1
A model of the crystal structure (assuming the *C*2/*m* space group) in the [203] direction is accompanied by the CBED pattern in the same direction. The mirror plane in the structure is evident in the zero and higher-order Laue zones. The zero-order Laue zone (ZOLZ) component shows the expected 2*mm* projected symmetry of the crystal structure in the [203] direction. Crosses indicate the exact zone axis.

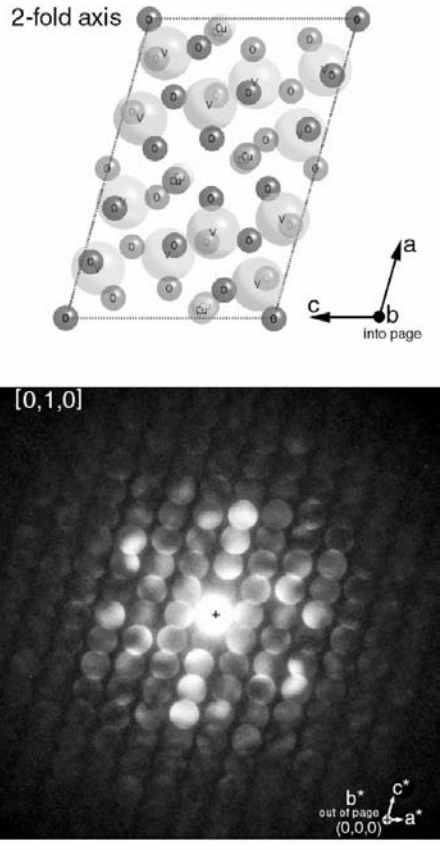

Figure 2
The *C*2/*m* structural model is viewed along the short *b* axis in the structure and the complementary ZOLZ CBED pattern shows twofold symmetry. The higher-order Laue zones (HOLZ) were too weak to be captured and out of the field of view due to their large distance from the ZOLZ. This pattern suggests twofold projected crystal symmetry along the [010] direction, the cross indicating the exact zone axis.

Both Figs. 1 and 2 have a black cross to show where the exact zone axis is. In both patterns the crosses do not coincide exactly with the centre of the incident beam. These very small misalignments change the position of the features within each of the discs relative to the corresponding features in their symmetry-related counterparts. This effect is very small, but must be taken into account when judging the integrity of the symmetries observed in both patterns. In Fig. 2 the exposure has been maximized to reveal a larger angular range in the intensity distribution within the CBED pattern. Many of the weakly excited reflections show twofold relationships, although very close inspection may reveal extremely subtle symmetry breaks. These are, however, at the very limits of detection and it is difficult to say whether these are due to the crystal structure or the limits of the instrumentation.

2.4. Deviations from *C*2/*m* detected by CBED

Some patterns taken at the [010] zone axis in different crystals exhibit symmetry breaks and an example collected at 160 KeV is given in Fig. 3(*a*). This shows a lack of the twofold symmetry seen in Fig. 2. Accompanying this pattern is one taken along the [101] direction, shown in Fig. 3(*b*), that should have 2*mm* symmetry in the ZOLZ part of the pattern, but is clearly only *m* in both ZOLZ and HOLZ.

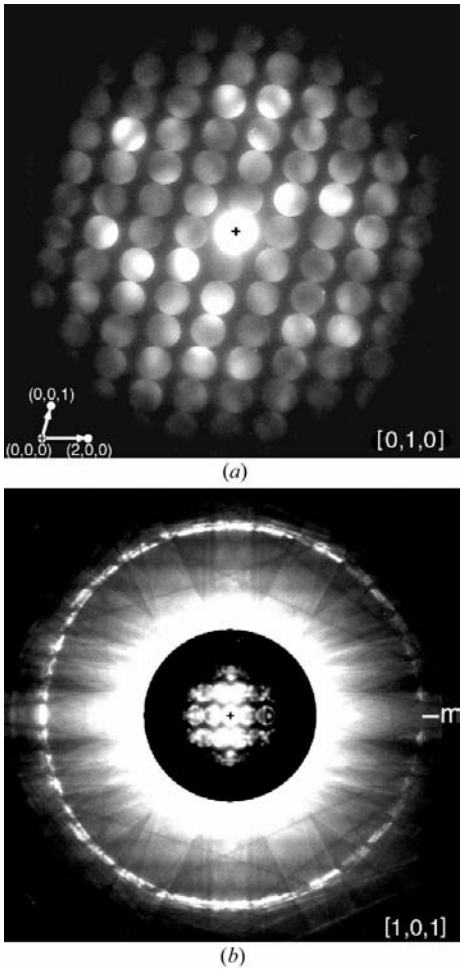

Figure 3
Examples of CBED patterns taken in different crystals showing breaks from the symmetries expected from a *C*2/*m* model: (*a*) a pattern at the [010] zone axis, showing no twofold symmetry; (*b*) a [101] zone-axis pattern showing only *m* and no 2*mm* symmetry in the ZOLZ. Crosses indicate the exact zone axis.

Crystal thickness measurements by CBED pattern-matching using a modified version of the *RefineCB* program by Zuo (Zuo, 1993; Spence & Zuo, 1992) showed that the patterns containing symmetry breaks came from thicker regions of crystal than those where the elements of *C*2/*m* were preserved. It also became apparent from this aspect of the investigation, as well as *in situ* observations, that the twofold axis is destroyed before the perpendicular mirror (*ac* plane) as specimen thickness is increased.

3. Results and discussion

The highest symmetry observed by CBED in the $Cu_{0.63}V_2O_5$ structure was *C*2/*m*, conclusively exhibited by the thinner regions of the specimens from which patterns were collected. As crystal thickness increased in the CBED experiments, the symmetry reduction in the crystal structure progressed as follows: $C2/m \rightarrow Cm \rightarrow C1$. No evidence of *C*2 symmetry was found in any of the regions of the specimen examined by CBED.

If the observed symmetry reductions were the result of insufficient averaging over polar domains or a lack of Cu-atom ordering/stoichiometry, then these effects would be more pronounced in thinner regions of the specimen, counter to the present results. The present CBED observations suggest that crystal defects such as stacking faults or dislocations (possibly introduced during crushing for TEM specimen preparation) are more likely to be responsible for the reductions in symmetry as the probability of encountering such defects within the diffracting volume increases with greater specimen thickness. No attempts to image or characterize such flaws were made in the present experiments.

The present CBED results, however, do conclude that the smallest volumes of $Cu_{0.63}V_2O_5$ probed, which are least likely to contain mechanically induced flaws, have a centrosymmetric *C*2/*m* crystal structure. This is therefore the most valid model for performing the crystal structure refinements using the X-ray diffraction data. The tests performed on the X-ray data do not contradict this conclusion.

After establishing the three-dimensional symmetry, the crystal structure of $Cu_{0.63}V_2O_5$ was refined in the *C*2/*m* space group using the X-ray diffraction data at 9.6 K. A full-matrix least-squares procedure, minimizing the quantity $w(F_o - F_c)^2$ with $w = 1/\sigma^2$, was utilized in *Xtal*3.7 (Hall *et al.*, 2000). Inspection of the residual electron density map with only the Cu1 component subtracted (Fig. 4*a*) shows two strong maxima, suggesting that the Cu atoms are distributed over two crystallographic positions. The Cu2 position was refined and the strong maxima disappeared in Fig. 4(*b*) where both copper components were subtracted. Similar split positions were also found in $Fe_xV_2O_5$ by Permer & Ferey (1994). Temperature changes have no significant effect on the crystal structure. This

Table 4
Selected bond lengths (Å) for $Cu_{063}V_2O_5$ (96 K).

Cu1—Cu2^{i}	0.292 (7)	Cu2—Cu2^{i}	0.28 (1)
Cu1—O4	1.877 (3)	Cu2—O4	1.841 (4)
Cu1—O6^{ii}	2.180 (2)	Cu2—O6^{ii}	2.225 (7)
Cu1—O8^{iii}	1.930 (3)	Cu2—O8^{iii}	1.871 (4)
V1—O2	2.2214 (7)	V2—O3^{iv}	1.8863 (2)
V1—O2^{iv}	1.8811 (2)	V2—O5	2.1747 (7)
V1—O3	1.9864 (8)	V2—O6	1.6577 (8)
V1—O4	1.6219 (7)	V3—O5	1.7827 (7)
V1—O5	1.9390 (8)	V3—O7	1.9808 (8)
V2—O1	1.8187 (2)	V3—O7^{v}	1.9004 (3)
V2—O2	2.2479 (8)	V3—O8	1.6377 (7)

Symmetry codes: (i) $x, -y, z$; (ii) $x+\frac{1}{2}, y+\frac{1}{2}, z$; (iii) $-x+1, -y, -z+1$; (iv) $-x+\frac{1}{2}, -y+\frac{1}{2}, -z$; (v) $-x+\frac{1}{2}, -y+\frac{1}{2}, -z+1$.

suggests that the strong peaks in the residual electron density map near the Cu1 positions are more likely to be static than dynamic as anharmonicity is expected to be insignificant at 9.6 K.

The final structure refinement parameters including agreement factors, $R = \Sigma||F_o| - |F_c||/\Sigma|F_o|$, $wR = \{\Sigma[w(F_o^2 - F_c^2)^2]/\Sigma[w(F_o^2)^2]\}^{1/2}$ and $S = \{\Sigma[w(F_o^2 - F_c^2)^2]/(n-p)\}^{1/2}$, are cited in Table 1, where n is the number of reflections and p is the total number of parameters refined. The atomic coordinates and anisotropic displacement parameters have been deposited. Table 4 presents selected bond lengths in the structure.

The atomic displacement parameters for the lower occupancy Cu2 site are greater than those for the higher occupancy Cu1 site. This is probably related to the higher disorder of the Cu2 position. A similar trend was observed for other vanadium oxide bronzes with split crystallographic sites for the M metal (see *e.g.* Déramond *et al.*, 1994; Permer & Ferey, 1994). Further analysis of the atomic displacement parameters for other β (β') bronzes including β-$Na_xV_2O_5$ (Ozerov *et al.*, 2001) shows that the V2 atoms exhibit greater and more anisotropic [U^{11}(V2) > U^{33}(V2) > U^{22}(V2)] displacement parameters compared with the V1 and V3 atoms. It seems that the V2 atoms are less restricted in the *ac* plane, because they form a two-leg ladder composed of corner-shared octahedra along the *b* axis in contrast to the V1 and V3 atoms which form a zigzag-type double chain composed of edge-shared polyhedra. This anisotropy of the V2 parameters is more pronounced in the present structure of β'-$Cu_{0.63}V_2O_5$. The present (Table 1) and recent temperature studies of vanadium bronzes including β'-$Cu_{0.65}V_3O_5$ (Yamaura *et al.*, 2002) showed that the *a* and *c* axes shrank monotonically, whereas the *b* axis was almost constant from 300 to 20 K. It was also suggested that the V2 atoms can move transversely to the V2 ladder forming superstructural modulations. The most recent X-ray power diffraction characterization of β'-$Cu_{0.66}V_2O_5$ under pressure (Yamaura *et al.*, 2004) revealed that the length of the *b* axis remained constant with increasing applied pressure, while the other axes decreased monotonically with greater linear compressibility in the *a*-direction than in the *c*-direction. The anisotropic dimensional changes of Cu-bronzes involving the structural deformations of the V2 ladder under pressure were related to the pressure-induced superconductivity in the Cu-bronzes. These results are consistent with the high anisotropy of the V2 atomic displacement parameters observed in the present structure.

Further comparison of β'-$Cu_{0.63}V_2O_5$ and β-$Na_{0.28}V_2O_5$ (Ozerov *et al.*, 2001) structures shows that the V—O framework is quite similar in the two compounds (Figs. 5*a* and *b*), as expected. In the sodium compound, the Na atoms occupy only

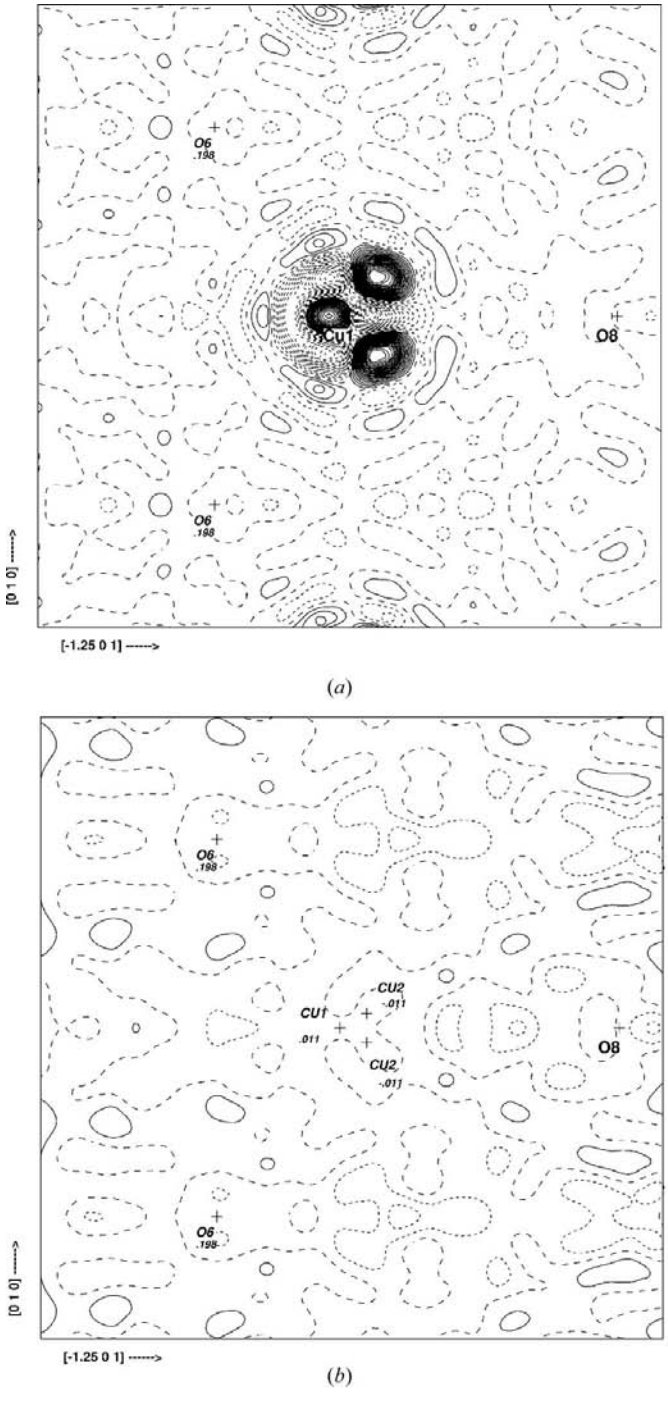

Figure 4
The residual electron density maps for the copper bronze with (*a*) only the Cu1 atoms subtracted (the two remaining Cu2 maxima are observed) and (*b*) all Cu atoms subtracted.

half of the 4(*i*) positions in an ordered or disordered manner, probably due to the large sodium ion radius. However, the Cu atoms in the *C*2/*m* space group, contrary to the sodium compound, were divided over two crystallographic sites: the Cu1 atoms occupy the 4(*i*) position and the Cu2 atoms occupy the 8(*j*) position with populations of 0.429 (14) and 0.254 (7), respectively (Table 4). Thus, these population parameters correspond to the value of $x = 0.63$ for the $Cu_xV_2O_5$ unit. It seems that the smaller size of the Cu ions ($\sim$ 0.9 Å for both Cu^+ and Cu^{2+}) helps Cu occupy additional positions. The distance between the two Cu2 atoms along the *b* axis is 0.28 (1) Å and the Cu1—Cu2 distance is 0.292 (7) Å (Table 4). The metal-ion size seems to be critical in the formation of either β- or β'-bronzes. Indeed, across the series of vanadium oxide bronzes studied so far, the β'-phase is formed when the *M* ionic radii are less than 1 Å, whereas for larger *M* radii the β-phase is dominant.

The Na and Cu bronzes also differ with regard to the Na and Cu positions in the O6 prisms. Figs. 6(*a*) and (*b*) depict the oxygen coordination prisms with respect to the metal positions for Na and Cu bronzes, respectively. It is remarkable that the Cu atoms are not only moved from the prism centres to their upper faces by *b*/2, but are also shifted out of the prisms forming CuO4 tetrahedra with distances given in Table 4.

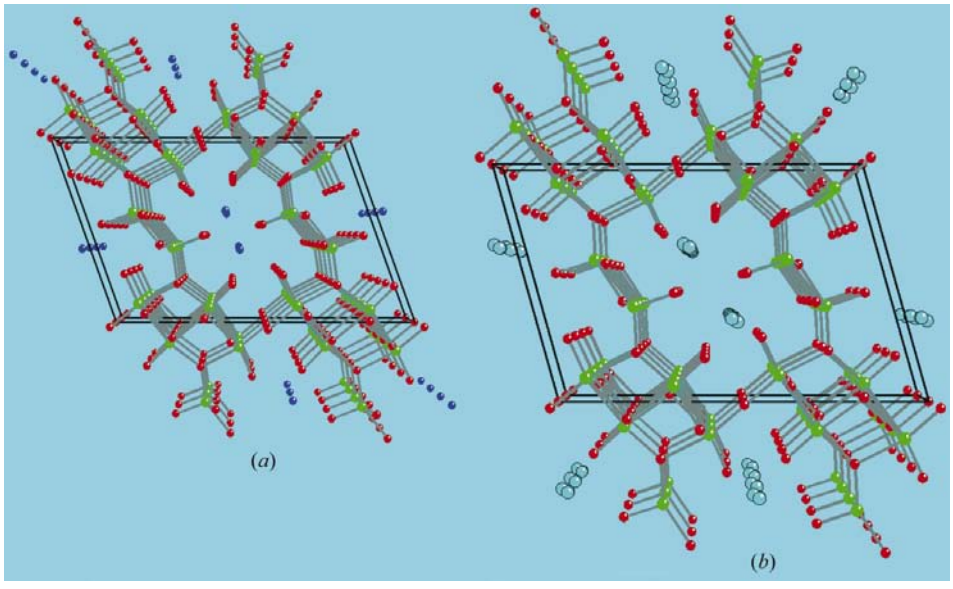

Figure 5
The V—O framework in (*a*) the sodium and (*b*) the copper bronzes.

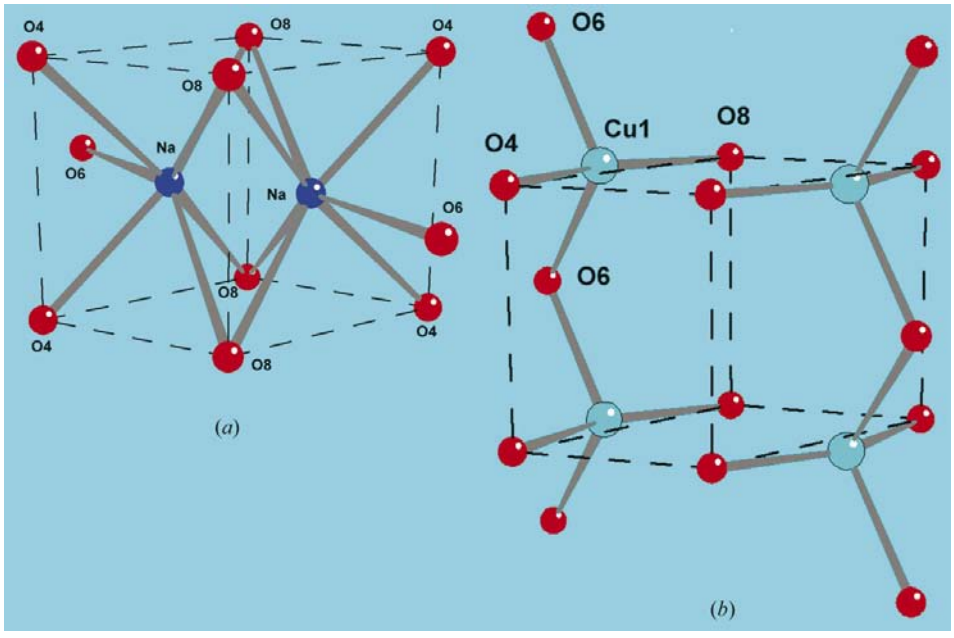

Figure 6
Oxygen coordination in (*a*) the sodium and (*b*) the copper bronze, only Cu1 is shown.

Since there are three types of vanadium ions (V1, V2 and V3), we have attempted to apply the valence bond (VB) approach (Brese & O'Keeffe, 1991; Brown & Altermatt, 1985) in order to assign a formal valence to these ions. The interatomic distances from our present and previous (Ozerov *et al.*, 2001) reports have been used in the VB calculations. The conventional R_{ij} value of 1.803 for V^{5+} has been used. The valences of the three V atoms were estimated as follows: V1 = 4.976, V2 = 4.954 and V3 = 4.976. The difference between the values lies within the uncertainty of the analysis. The application of the VB method is limited to the present system with strongly distorted V—O polyhedra and highly correlated electrons, where the strong electron interactions determine the type of ground state of the cation. Nevertheless, the lowest valence is estimated for the V2 ion, which appears to be the most charged vanadium ion from the multipole analysis of the electron density in the sodium bronze compound (Ozerov *et al.*, 2001). Furthermore, Yamaura *et al.* (2002) proposed that the V2 atoms are strongly involved in the charge ordering in the vanadium bronzes.

4. Conclusion

In the end, we conclude that the 9.6 K single-crystal X-ray studies of β'-$Cu_{0.63}V_2O_5$ showed neither convincing evidence supporting the non-centrosymmetric structure nor

symmetry breaking superstructure reflections at this low temperature. The centrosymmetric space group *C*2/*m* symmetry with two Cu crystallographic sites has been assigned based on room-temperature CBED studies and initial structural refinements using the X-ray data. The final structural refinements showed a higher anisotropy of the V2 atomic displacement parameters. This can be related to charge ordering and anisotropic structural changes involving the V2 atoms observed under pressure and at low *T*, which are in turn associated with pressure-induced superconductivity.

The single crystal of the copper bronze was kindly supplied by Professor Y. Ueda. We would like to thank Dr A. W. S. Johnson for valued discussion of CBED results.

References

Abrahams, S. C., Schmalle, H. W., Williams, T. A., Reller, F. L., Widmer, D., Bednorz, J. C., Spreiter, R., Bosshard, C. & Günter, P. (1998). *Acta Cryst.* B**54**, 399–416.

Brese, N. E. & O'Keeffe, M. O. (1991). *Acta Cryst.* B**47**, 192–197.

Brown, I. D. & Altermatt, D. (1985). *Acta Cryst.* B**41**, 244–247.

Déramond, E., Savariault, J.-M. & Galy, J. (1994). *Acta Cryst.* C**50**, 164–166.

Flack, H. (1983). *Acta Cryst.* A**39**, 876–881.

Flack, H. & Bernardinelli, G. (2000). *J. Appl. Cryst.* **33**, 1143–1148.

Galy, J., Lavaud, D., Casalot, A. & Hagenmuller, P. (1970). *J. Solid State Chem.* **2**, 531–543.

Goodman, P. (1975). *Acta Cryst.* A**31**, 804–810.

Goodman, P. (2001). *International Tables of Crystallography*, 2nd Ed., edited by U. Samueli, Vol. B, pp. 285–306. Dordrecht: Kluwer Academic Publishers.

Hall, S. R., du Boulay, D. J. & Olthof-Hazekamp, R. (2000). *Xtal*3.7. The University of Western Australia.

Hardy, A., Galy, J., Cashalot, A. & Pouchard, M. (1965). *Bull. Soc. Chim. Fr.* pp. 1056–1065.

Kato, K., Takayama-Muromachi, E. & Kanke, Y. (1989). *Acta Cryst.* C**45**, 1845–1847.

Ozerov, R. P., Gol'der, G. A. & Zhdanov, G. S. (1957). *Kristallographia*, **2**, 217–225 (in Russian).

Ozerov, R. P., Streltsov, V. A., Sobolev, A. N., Figgis, B. N. & Volkov, V. L. (2001). *Acta Cryst.* B**57**, 244–250.

Permer, L. & Ferey, G. Z. (1994). *Z. Kristallogr.* **209**, 413–417.

Popovic, Z. V., Konstantinovic, M. J., Moshchalkov, V. V., Isobe, M. & Ueda, Y. (2003). *J. Phys. Condens. Matter*, **15**, L139–L145.

Savariault, J.-M., Deramond, E. & Galy, J. (1994). *Z. Kristallogr.* **209**, 405–412.

Shacklette, L. W., Low, T. R. & Townsend, L. (1988). *J. Electrochem. Soc.* **135**, 2669–2674.

Shmueli, U. & Wilson, A. J. C. (1993). *International Tables of Crystallography*, edited by U. Samueli, Vol. B, pp. 184–200. Dordrecht: Kluwer Academic Publishers.

Smirnova, O. A., Michailova, A. M. & Seryanov, Yu. V. (2003). *Russ. J. Electrochem.* **39**, 1173–1177.

Spence, J. C. H. & Zuo, J. M. (1992). *Electron Microdiffraction*, pp. 151–152. New York, London: Plenum Press.

Streltsov, V. A. & Zavodnik, V. E. (1989). *Sov. Phys. Crystallogr.* **34**, 824–828.

Wadsley, A. D. (1955). *Acta Cryst.* **8**, 695–699.

Yamauchi, T., Ueda, Y. & Môri, N. (2002). *Phys. Rev. Lett.* **89**, 057002–057004.

Yamaura, J.-I., Isobe, M., Yamada, H., Yamauchi, T. & Ueda, Y. (2002). *J. Phys. Chem. Solids*, **63**, 957–960.

Yamaura, J., Yamauchi, T., Ninomiya, E., Sawa, H., Isobe, M., Yamada, H. & Ueda, Y. (2004). *J. Magnet. Mag. Mater.* **272–276**, 438–439.

Ueda,Y., Isobe, M. & Yamaguchi, T. (2002). *J. Phys. Chem. Solids*, **63**, 951–955.

Zuo, J. M. (1993). *Acta Cryst.* A**49**, 429–435.